

Loss Processes at Elevated Temperature

By Rachel Umbel

Adviser: Dr. Iain Martin

University of Glasgow

Scotland, United Kingdom

Abstract:

Through University of Florida International Research Experience for Undergraduates, I worked with the IGR group at University of Glasgow during the summer of 2009. The aim of my project was to explore the mechanical loss processes in dielectric mirror coatings, which are used in gravitational wave detectors, at elevated temperatures. This was achieved by measuring the ring downs of coated and uncoated cantilever structures in a specially designed vacuum chamber and calculating their mechanical losses as well as the thermo elastic losses for the various cantilevers. In addition, the coated and uncoated cantilevers mechanical losses were measured at temperatures up to 500K.

1. Introduction:

University of Glasgow's Institute for Gravitational Research group is part of an international collaboration in the search for gravitational waves. Gravitational waves were first predicted by Einstein Theory of Relativity. A gravitational wave could be compared to an electromagnetic wave. One difference between the two waves is an electron charge can be positive or negative where mass can just be one sign. In this difference, an electromagnetic wave is dipole in nature, where a gravitational wave is quadruple. Thus, a gravitational wave is harder to detect, as a gravitational wave is only produced when a mass accelerates and changes shape as pictured on a two-dimensional field with one dimension time and one space. Indirectly, gravitational waves have been detected through binary pulsars, but they have remained undetected to date. [1]

There are currently limitations on the present interferometers to detect gravitational waves. It is predicted that the signals of the gravitational waves will be small. A previous letter states that gravitational wave detectors on earth can detect a frequency range of 10 to 10^4 Hz. At this frequency, the strain signals will typically be less than 10^{-21} over bandwidths of a few hundred Hertz. [2] In addition, background noise makes the detection of the signals more challenging. At low frequencies, seismic noise is the limiting factor; this is frequencies up to about 10Hz. At higher frequencies lasers are the limiting factor due to the photo-electron shot noise. At around 30Hz to 400Hz, thermal noise is the main limiting factor in interferometer gravitational wave detectors. The thermal noise in these detectors is mainly associated with the mirror masses and their suspensions within the detectors. Currently, the mirror masses are made from fused silica, although possible improvements may use crystalline materials which would be suitable for cooling. [4]

2. Background:

Thermal noise forms an important limit to the sensitivity of km-scale interferometer detectors, so recent work has been aimed to reduce this thermal noise. Thermal noise appears in two forms of Brownian noise and thermo elastic thermal noise. The thermal noise can be described as "A result from the thermal energy of the atoms and molecules in the test masses and suspensions." [2] Brownian noise is related to the level of internal friction in the system and thermo elastic thermal noise is from the statistical temperature fluctuation in the system. Thermal noise, in relation to the dielectric mirror coating used in gravitational wave detectors, can be difficult to calculate, but thermal noise is related to the total mechanical loss of a system. From the mechanical loss of the system, the thermal noise from the suspended mirror can be calculated. [2] [6]

Material for the test masses and suspensions has been currently reviewed. Fused silica is used in all current interferometers. Fused silica has suitable optical properties as well as a low mechanical dissipation and thus low Brownian thermal noise. [2] In addition, the thermo elastic thermal noise in silica substrates is low as due to the low coefficient of thermal expansion. [2 as cited in 3] Another concern is the temperature

dependence of the materials used. Low temperature detectors seek to reduce the thermal noise, currently low temperature detectors are used just for bar detectors and not interferometers although this is a possibility. Fused silica would not be suitable to use in low temperature detectors as it has a dissipation peak around 40K. Other substrates were suggested such as sapphire or silicon which are currently being studied. [2]

Work has been done to reduce the effects of the mechanical dissipation, and thus the thermal noise, in the dielectric mirror coatings. The coating is made from a high refractive material alternated with a low refractive layer. A common coating is silica with alternating layers of tantala where the dissipation is dominated by the tantala. The loss in the coatings was found to be at a significant level. It was found that the majority of the dissipation in the coatings is due to the high refractive coating which was tantala. A solution is to dope the high refractive material with another material to decrease the losses of it. The dissipation could be reduced by doping tantala with TiO₂. Further areas of interest were noted that fused silica dissipation will increase as temperature is decreased from room temperature. There is a broad mechanical dissipation peak centred around 40-60K as mentioned early. Therefore, as mentioned in previous research and as the goal of this research, it is of considerable interest to explore the temperature depended of dissipation in coatings materials. [5]

3. Theory:

3.1 Calculation of Bending Modes

Initially, the n th bending modes of different cantilevers are able to be calculated by the following formula:

$$\omega = (k_n L)^2 (Y/\rho)^{1/2} a / (2 \cdot 3^{1/2} L^2) \quad (1)$$

With thickness a , length L , Young's Modulus Y and density ρ , and where $k_n L = 1.875$ ($n=1$), 4.694 ($n=2$), 7.853 ($n=3$), 10.996 ($n=4$) and 14.125 ($n=5$) and for $n > 5$, $k_n L$ is equal to $(2n-1) \pi / 2$ [6]. This formula provided the resonant modes for the bending modes, but not the torsional modes which were also studied. Further verification was also provided by a computer modelling program, ANSYS, discussed later.

3.2 Mechanical Loss

Furthermore, the mechanical loss which is also known as the mechanical dissipation was measured for each mode. The mechanical loss is the total loss for the system. The loss can be determined by a few different methods. The method employed in this paper was by using the ring downs of the cantilevers. Each resonant mode of the cantilever, ω , would be excited via the excitation plate in the chamber in turn. After the excitation, the cantilever would be allowed to oscillate until the resulting motion from the excitation decreased to almost stationary. The time dependent amplitude decay could be modelled in the following form [6]:

$$A(t) = A_0 e^{-\varphi(\omega_0) \omega_0 t / 2} \quad (2)$$

The loss is then found from the measurements of the amplitude of the decaying resonant motion as a function of time. Allowing alpha, α , to equal phi, ϕ , times angular frequency, ω , divided by two.[6] Thus

$$\tau = 1/\alpha = 2/(\phi \omega_0) = 2/2\pi f \phi = 1/(\pi f \phi) \quad (3)$$

Therefore,

$$\phi = 1/(\pi f \tau) \quad (4)$$

Another method is via the energy in the system is seen below:

$$\phi(\omega_0) = E_{\text{Dissipated}} / (2\pi E_{\text{stored}}) \quad (5)$$

where E_{stored} is the total energy stored in the vibrating system, and $E_{\text{Dissipated}}$ is the energy dissipated with each cycle of oscillation.

3.2.1 Loss in Coating

The loss was calculated for the coating of the coated cantilevers. In a coated cantilever, the thickness of the coating was very small in comparison to the cantilever; by this, the dissipation in the coating was small, as there was only a small amount of energy stored in the coating. The measured loss of the coated cantilever, $\phi(\omega_0)_{\text{coated}}$ is related to the loss of both the cantilever substrate and the intrinsic loss of the coating material. It can be calculated by [6]

$$\phi(\omega_0)_{\text{coated}} = \phi(\omega_0)_{\text{substrate}} + E_c/E_s \phi(\omega_0)_{\text{coating}} \quad (6)$$

Where E_c/E_s is the ratio of the energy stored in the coating layer to the energy stored in the cantilever substrate.

The energy ratio can be found via the bar of length L , thickness a , and width b , with a thin coating of thickness t on one surface and bent into an arc of circle of radius R . Thus, through substitution, the ratio of energy can also be shown as:

$$E_c/E_s = (3Y_c t) / (Y_s a) \quad (7)$$

From this relation, the coated loss formula can be written as,

$$\phi(\omega_0)_{\text{coating}} = (Y_s a) / (3 Y_c t) (\phi(\omega_0)_{\text{coated}} - \phi(\omega_0)_{\text{substrate}}) \quad (8)$$

3.3 Thermo elastic Dissipation

The thermo elastic dissipation was calculated for the different cantilever systems. Thermo elastic dampening is from an anelastic relaxation process related to the flow of heat in a material and arises from the coupling of temperature. As the bar bends in, that side of the cantilever heats up due to compression, as the heat flows from hot to cold, then the bar bends the other way which causes the first side to cool because of expansion. Furthermore, thermo elastic dissipation is frequency dependent and the peak frequency is related to the time taken for heat to diffuse across the thickness of a cantilever. Equation nine provided the calculated thermo elastic loss by employing

the dimension and material properties of the cantilever [6]:

$$\phi = (2 Y \alpha T) / (p C \tau) / (1 + \omega^2 \tau^2) \quad (9)$$

and

$$\tau = p C t^2 / ((\pi)^2 k) \quad (10)$$

4. Procedure

4.1 Design of System

An initial design of an apparatus which would allow the resolution of anelastic relation effects in evaporated metallic thin films and ion implanted surface layers of silicon is proposed by Berry and Pritchett. This would provide insight into the nature and behaviour of crystal defects at an atomic level, and is the best way to measure the vibration frequency. In recent years, the samples have become thinner. There are three main sources of external energy loss of air damping which at normal pressure can be much larger, transducer loss and support loss, which cannot be calculated independently [7]. In this experiment, air damping was minimized by operating at pressures below 10^{-5} mbar. To minimize support loss, the thin cantilevers were attached to thicker clamping blocks, thus reducing frictional energy loss in the clamp.

In order to measure the mechanical loss of the cantilevers and in turn the coatings, a vacuum chamber design was used. A cantilever sample was comprised of a clamping block as well as the cantilever. The clamping block on the cantilever was attached inside the chamber to the clamp base with a rectangular upper clamp block. The upper clamp block was tightened with two screws on each side. The clamp block was attached to a circular metal base which allowed it to be removed from the chamber. The excitation plate was positioned a few millimetres below the cantilever and was stabilized via a post. The voltage for the excitation plate was around 500V and provided by a high voltage amplifier. A mirror was positioned above the cantilever sample which a laser was aimed at. The laser bounced off the mirror onto the cantilever which the cantilever reflected to the detector. The detector used was a split photo diode detector. The chamber would be pumped down to pressures of magnitude to the negative seventh mbars.

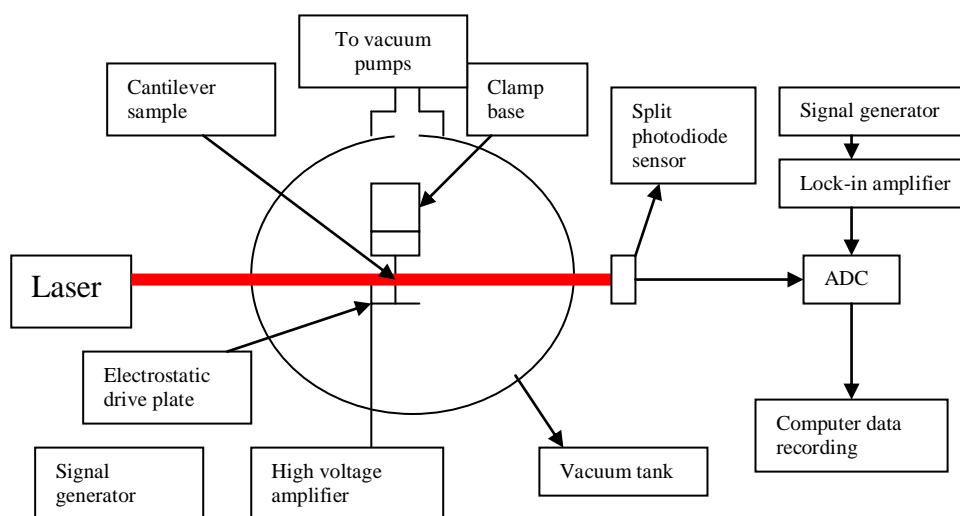


Figure 1: A schematic diagram of the experimental apparatus to measure mechanical loss of cantilever samples

4.1.1 The Design of the software

Multiple software programs were used in the measurement and calculation of the ring downs. The programs were written into Lab View. Brief overviews of their capabilities are outlined below.

1. The spectral scan was used to find the resonant modes. The desired range is entered as well as the voltage. The program will scan through the range to detect resonant modes. The detection is through the photo diode detector which measures the vibrations in the cantilever. An output graph of frequency versus amplitude is produced.
2. The 2nd channel cantilever program was used to measure the ring downs. The different resonant frequencies were entered in as well as desired excitation voltage. The program scanned through multiply resonant modes infinitely. The program records the scan as frequency versus amplitude, and the ring down is recorded as times versus amplitude of the cantilever.
3. The third program monitored the temperature of three temperature probes which are used inside the specially designed vacuum chamber. A third temperature probe was recently added to calibrate the heater.

4.2 Resonant Modes

4.2.1 Bending Modes

Initially, the cantilever was modelled using a simulation program of ANSYS. ANSYS allowed for the specifications of the cantilever which include, but not limited to the thickness, length, material and geometry, and would calculate the resonant modes for that cantilever. A design from ANSYS can be seen below. It is using a silica cantilever with a silica clamping block. The clamping block is 11 mm by 11mm with 1mm thickness. The cantilever is 45 mm by 5 mm and 110 microns thick. Furthermore, the diagram is fixed at the clamping block, to replicate the clamping block in the specially designed vacuum chamber.

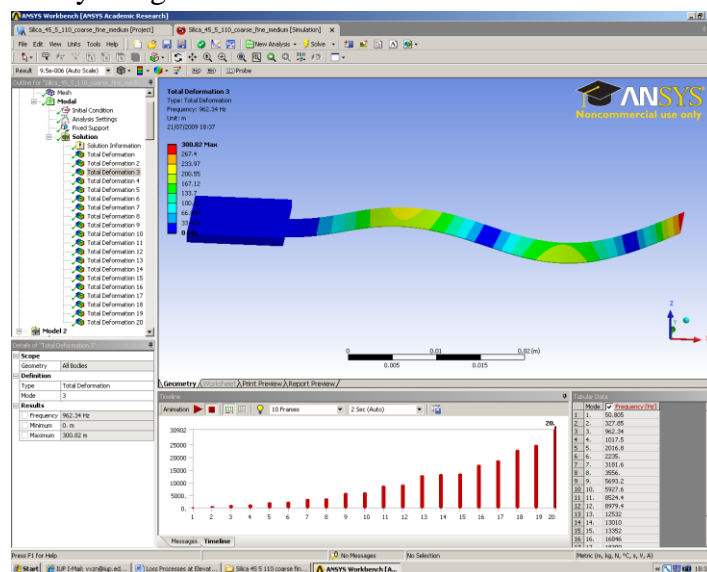


Figure2: Example of ANSYS program of a modelled silica cantilever for the third bending mode

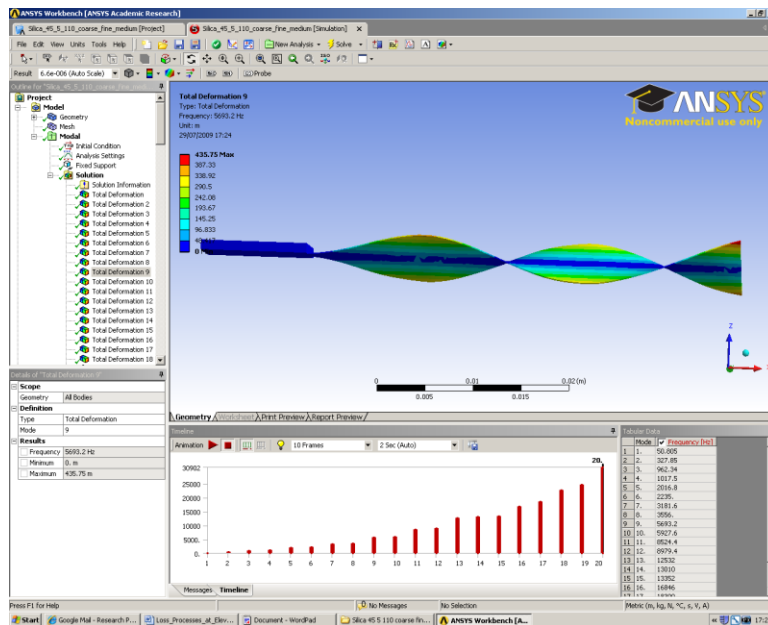


Figure 3: Example of ANSYS program of a modelled silica cantilever for the third twisting mode

ANSYS was further used in the coatings. ANSYS allowed a coating to be applied to a cantilever as well. The coating is added on top of the cantilever and the thickness can be chosen. From here, the resonant modes are also calculated with the user's desired geometry.

4.2.2 Torsional Modes

In addition to bending modes, torsional modes were also modelled via ANSYS. The torsional modes would tend to be at a higher frequency than the corresponding bending mode. There was no direct calculation for torsional modes, but the torsional modes would be predicted by ANSYS and verified by using the spectral scan to detect the resonant mode at the predicted frequency.

4.3 Verification of Thickness

The cantilever's thickness would be verified by the calculation of a bending mode. The 2 Channel Network Signal Analyzer would be scan over a small range of expected peak, to locate the fundamental mode. From the fundamental mode, the thickness was then calculated from equation (1). After the fundamental mode was found, the other modes could be estimated, and also used to verify the thickness. Often the expected thickness and actual thickness varied.

4.4 Mechanical Loss

The mechanical loss was calculated for each resonant mode by equation (4). The loss would be calculated with both the automatically generated tau value from LabView 2nd Channel Program as well as by hand with the saved results of the ring down. This was to ensure a best fit line and further verification of the program.

4.5 Thermo elastic Loss

In order to find the thermo elastic loss, first, the resonant modes had to be verified by using Lab View's spectral scan. It allowed the user to enter in the initial and final frequencies and find the resonant mode over various ranges. After the resonant mode was found, LabView's 2nd Channel cantilever program allowed the user to find the ring downs for each of the resonant modes. The computer would calculate the loss, but all the losses were verified by the user.

4.5.1 Temperature Dependence of Thermo elastic Loss

The temperature dependence of the thermo elastic loss was limited as the temperature dependence of many of the mechanical properties were not able to be located.

4.3 Heated Chamber

To reach temperatures of 400K, a specially designed heater box was created. The box was made out of aluminium foil four sheets thick. This box accommodated the laser beam via two holes in either side for the laser to shine through so not to impede the photo diode detector. A copper wire was attached to the clamp block and glued to the lid for thermal conductivity. Temperature sensors were added to the resistor as well as the clamping block to monitor the temperature during the heating process. The wires for the temperature sensors were four strands to reduce the resistance in them. In addition, a flat top lid was later used to minimize the interference with the wires and laser. An image is given below:

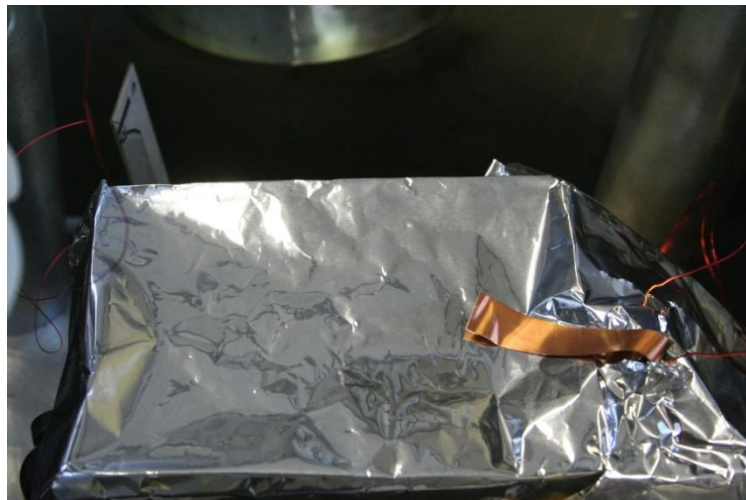


Figure 4: Image of heater box used in specially designed vacuum chamber

5. Experimental Results:

5.1 Non Heated Cantilever

5.1.1 Silicon Cantilever

The bending modes and ring downs were calculated for a 58.5 nm thick silicon sample. Initially, the bending modes were calculated for a 70 nm thick cantilever, after verifying the fundamental modes and a few other modes, the thickness was calculated to be an average of 58.5 nm. ANSYS was then used to predict the bending modes and torsional modes. Eighteen bending modes were detected for the silicon cantilever. The eighteenth was at 56784Hz. The loss was calculated for each of the modes. It was found that as the frequency increased, the loss increased as seen in Fig. 5.

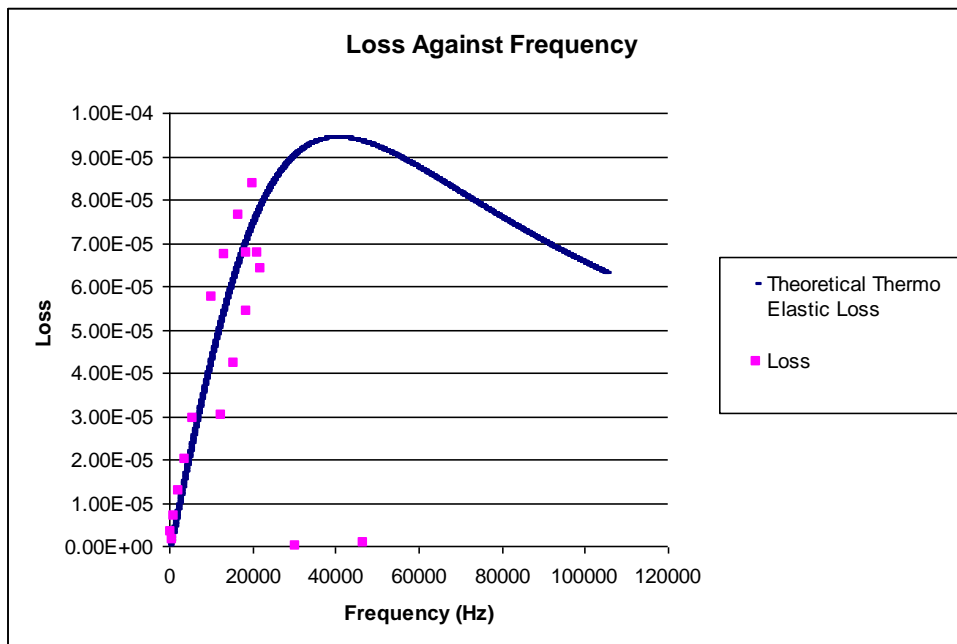


Figure 5: Comparison of the theoretical thermo elastic loss versus the frequency for a silicon cantilever and the measured loss values

At the lower frequencies, the loss is almost all due to thermo elastic dissipation. At the higher frequencies, there appears that some other loss is present as the thermo elastic loss is less than the total mechanical loss. Another interest to note is that some points fall below the expected curve. One reason for this could be due to they are not bending modes, but instead twisting modes. The average losses were around the order of magnitude of 10^{-5} to 10^{-6} . Another interesting occurrence was found at the last two bending modes of 30201 Hz and 56784 Hz, as these two losses were much lower than the expected trend; these results are questionable as no decay curve could be fit to the ring downs. A peak in the theoretical thermo elastic loss occurs at 40 KHZ, but the valid experimental results only reach up to around 25KHZ.

5.1.2 Silica Cantilevers

Four different silica cantilevers were tested. There were two laser fused silica cantilevers and two flame fused silica cantilevers tested. The silica cantilevers had a

wider clamping block than the cantilever which was unlike the silicon cantilevers. For all four of these cantilevers, the loss was fairly high.

5.1.2.1 Laser Fused Silica Cantilever

The laser fused cantilevers were designed by welding the clamping block to the cantilever with a laser. The laser fused samples were more even than the flame fused, but a distinct edge remained at the bonding site. For the first laser fused silica sample, four bending modes were found. The loss was around 10^{-5} with increasing loss as frequency increased. There was a lot of difficulty finding the resonant modes for these cantilevers. For the second laser fused silica sample, the loss average was 10^{-5} , and five bending modes were detected. The results were surprisingly high as seen in Fig. 6.

5.1.2.2 Flame Fused Silica Cantilever

For the first flame fused silica sample, only a single bending mode at 1510Hz was found with loss of magnitude of 10^{-6} . After tightened the clamp, this was still the only detectable bending mode. The second flame fused silica sample, the loss was 10^{-5} to 10^{-6} for four frequencies.

5.1.2.2 Silicon Clamping Block Cantilever

A final cantilever of silica bonded to silicon clamping block was also tested. The results from this cantilever were messy, as some of the points did not follow the trend of increasing frequency, increasing loss.

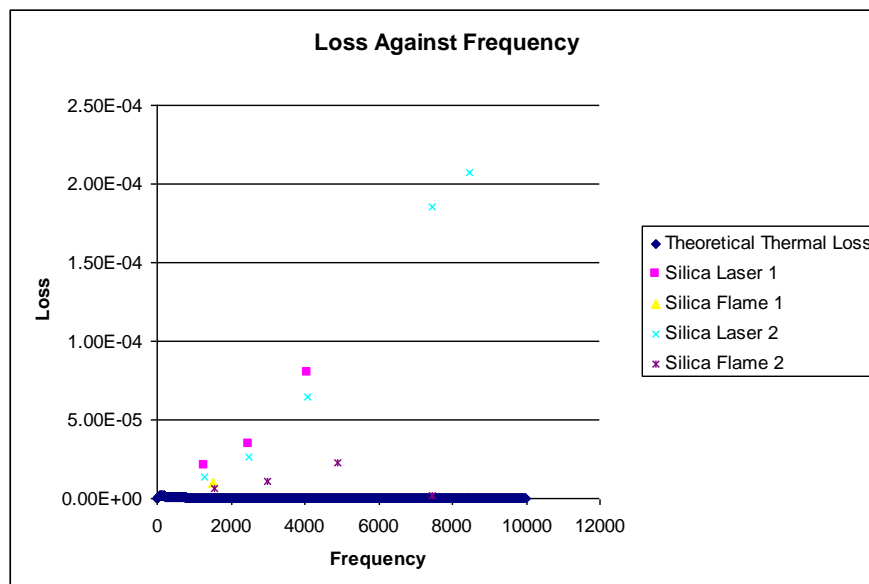


Figure 6: The large loss in the silica cantilevers can be seen above as their mechanical losses are all higher than the expected theoretical thermo elastic loss.

5.2 Heated Cantilever

The cantilever's ring down and resonant modes were also found at elevated temperature. The temperature distribution within the chamber was found to vary quite a bit when heated. There was over a 100 degrees temperature difference between the cantilever tip and the clamp. This provided a limit to the temperature the cantilever could reach. With the heater box, the difference was reduced, as well as the cantilever could achieve higher temperatures. It was found that with the heater box, there would be around a 25% increase from the cantilever to the clamp, this became stable at higher temperatures, at lower temperatures the difference varied more. At the clamping block of 309K, the heater at 370K and the cantilever at 327K. At a higher temperature, the differences became more evidence with the heater at 480K, the clamp at 420 and the cantilever at 320K, these results were taken from July 13. Further verification was done to insure that the temperature sensor was not affected by the heat conductivity along the wires.

After initial temperature measurements were done, the chamber was vented, and the wires were positioned out of contact with any possibly contamination as to test whether there was any heat conductivity along the wires. No evidence of any heat conductivity was found. Figs. 7 and 8 represent the comparison of before and after the heater box was installed. Fig. 7 is the temperature of the heater, clamp and cantilever prior to the heater box with the voltage at 11.0 Volts and 2.36 Amps. Fig. 8 is the temperature of the heater, clamp and cantilever after the installation of the heater box. This trial was run at a voltage of only 8.0 Volts and 1.18 Amps, and the temperatures achieved were significantly higher than the non-heater box trial. The heater box reached temperatures of 608K for the heater, with the clamp 455K and the cantilever 513K when the voltage was 11.4 with 2.90 amps. The non-heater box only managed 424K, 376K, 339K for the heater, clamp and cantilever respectively with higher current and voltage of 3.8 amps and 12.2 volts. The placement of the sensor was also studied as seen in Fig. 9 and 10.

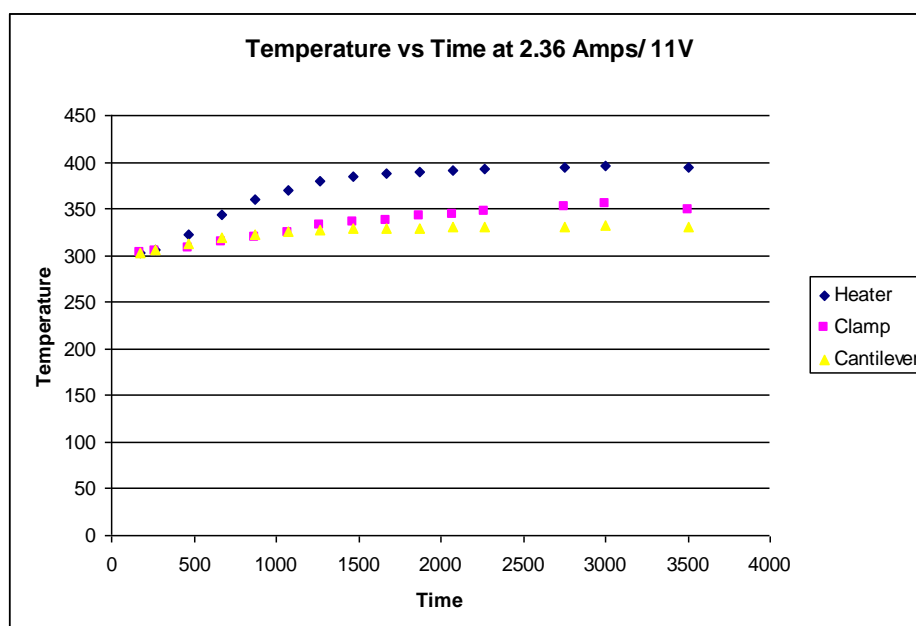


Fig. 7: Heating the chamber, no heater box

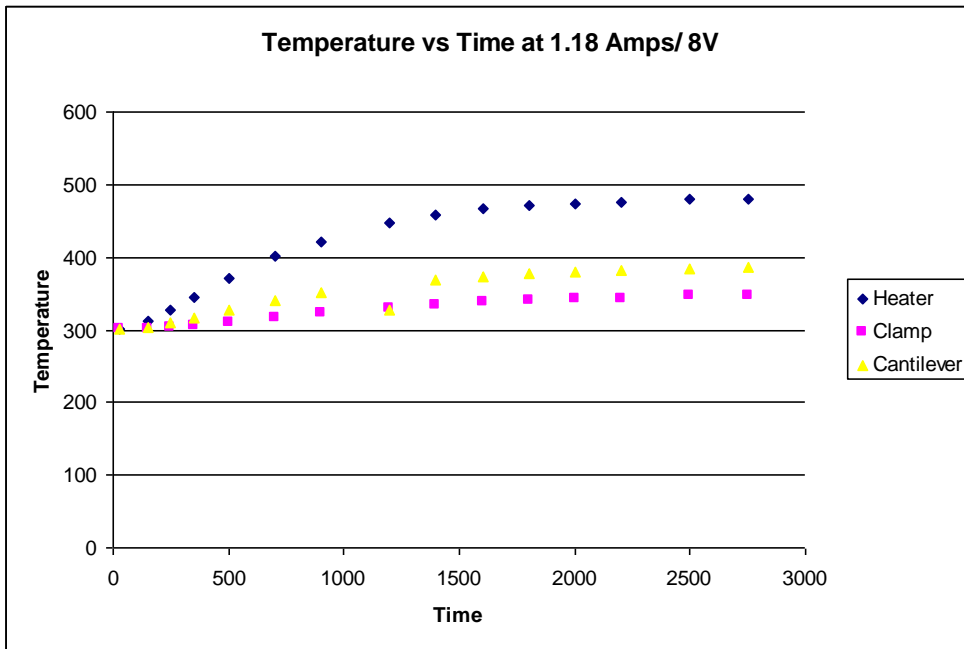


Fig. 8: Heating the chamber, heater box

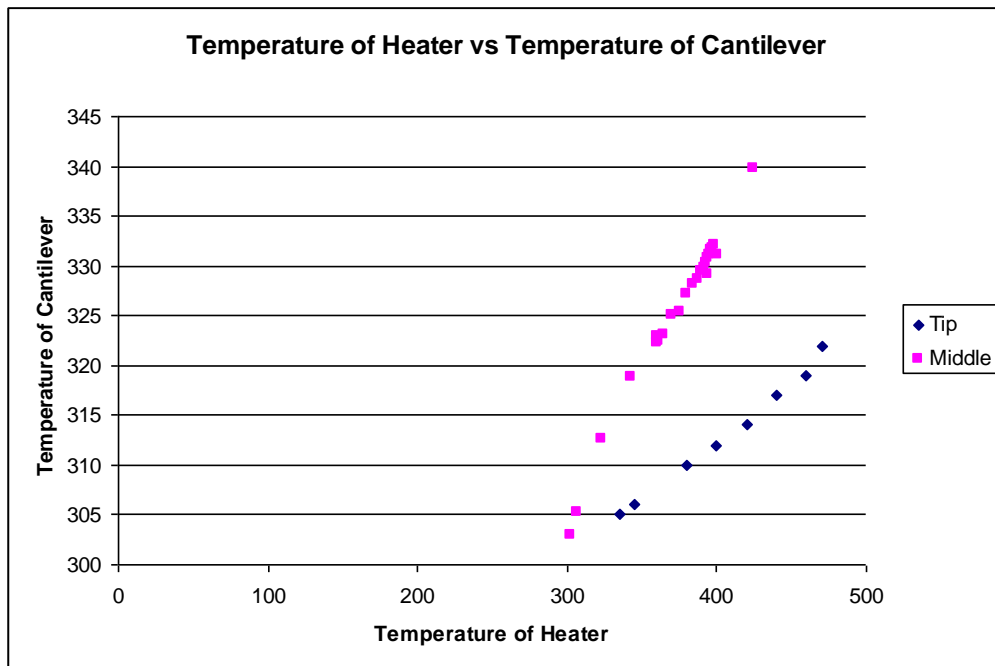


Figure 9: Comparison of the temperature of the heater to the temperature of the cantilever with the sensor placed on the tip and then the middle of the cantilever

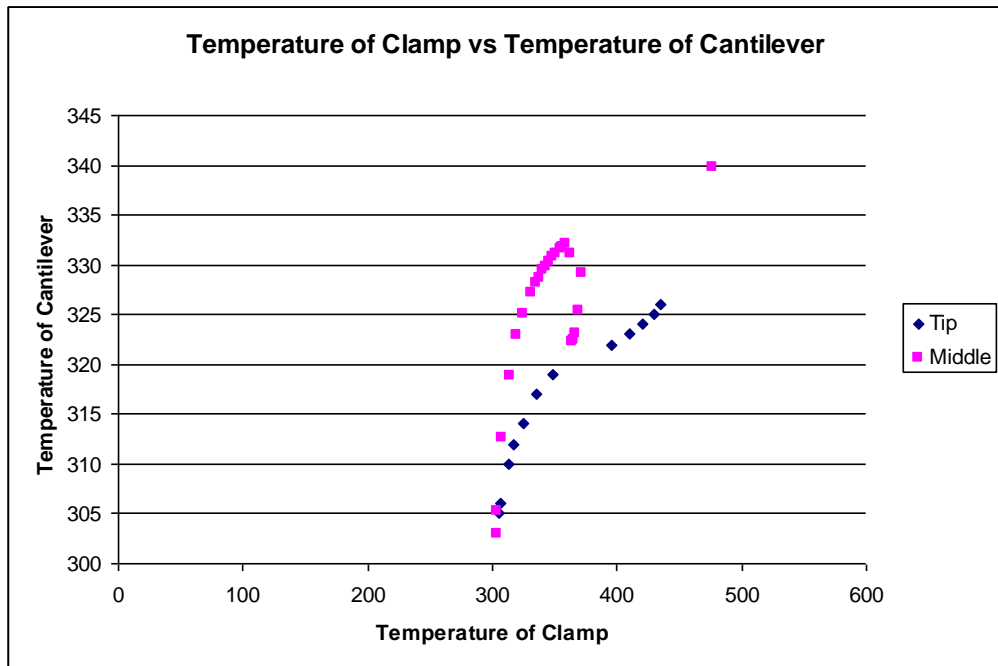


Figure 10: Comparison of the temperature of the clamp compared to the temperature of the cantilever with the sensor at the tip of the cantilever and the middle of the cantilever

5.2.1 Silica Ribbon Cantilever

A silica cantilever ribbon was used as the sample for heating. Measurements were taken at varying temperatures, as well as different methods of heating. Initially, the chamber was heated, and then cooled in increments of 10 or 20 degrees. Measurements were also taken as the chamber was heated by 10 or 20 degrees at a time. The ranges of temperatures are from 300K to 500K. It appears that 500k is the limiting temperature for the design. The average loss of these temperatures can be seen in Figs. 11 to 16. To date, over 900 samples have been taken. As the temperature increases, the loss tends to increase. Also of note, was the screws in one particular trial over July 16 to July 17, 2009. After heating the silica ribbon, it was found that the screws had become loose. They were retightened, and the loss decreased by roughly one order of magnitude.

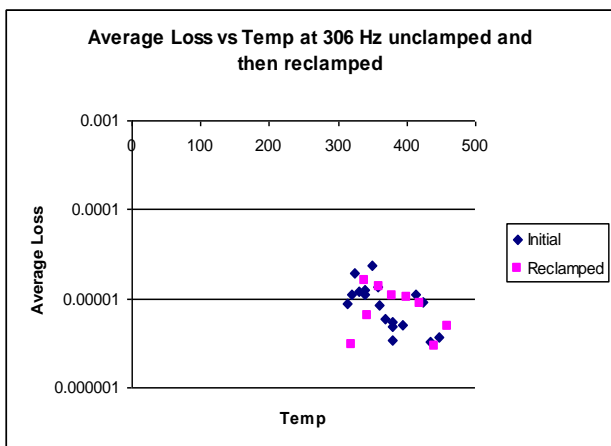


Fig. 11: Average Loss at 306 Hz

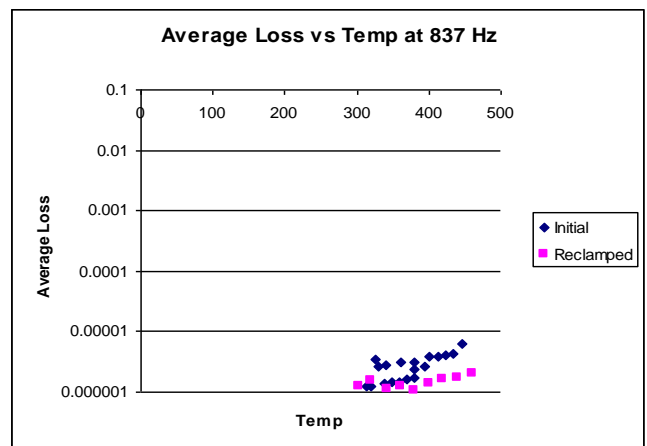


Fig. 12: Average Loss at 837 Hz

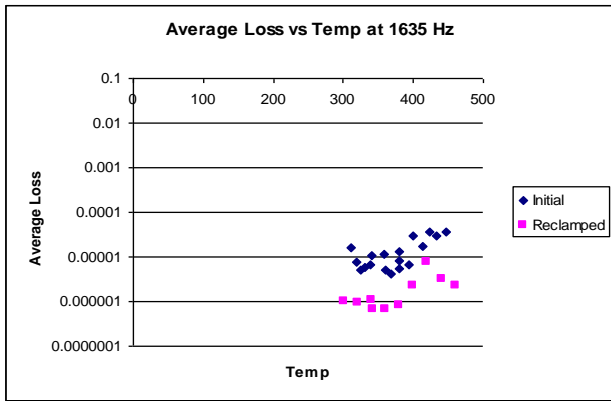


Fig. 13: Average Loss at 1635 Hz

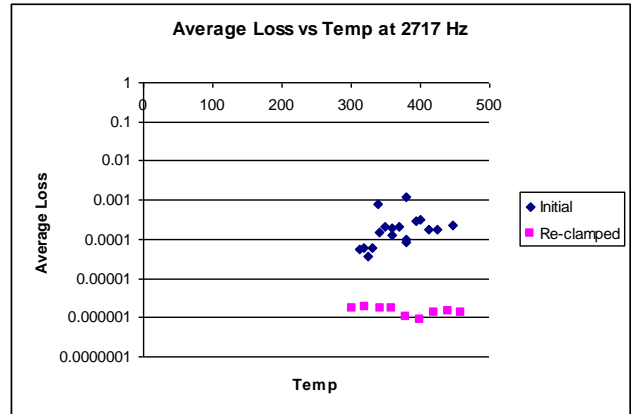


Fig. 14: Average Loss at 2717 Hz

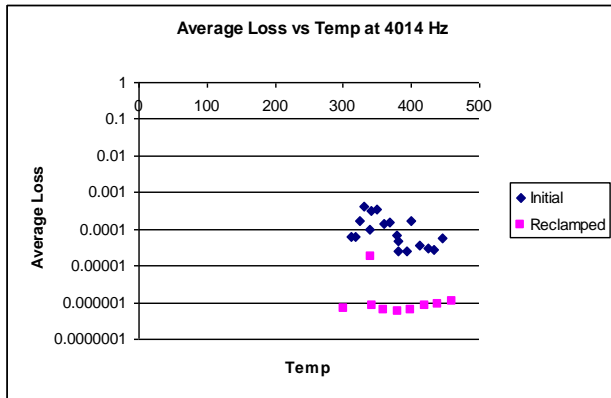


Fig. 15: Average Loss at 4014 Hz

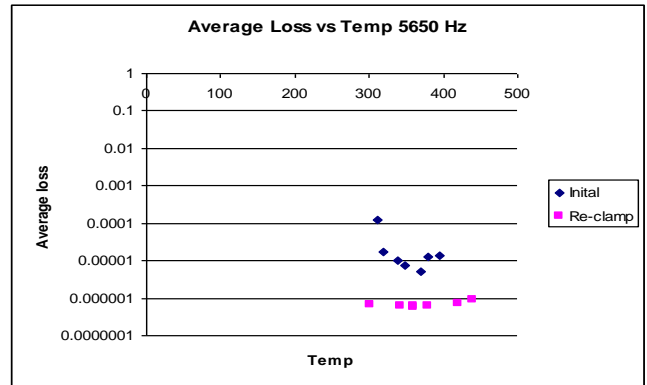


Fig. 16: Average Loss at 5650 Hz

5.3 Coated Cantilever

5.3.1 Non heated cantilever

A silica ribbon coated with 500nm of tantala was tested at room temperature. The resonant modes were found initially as well as the ring downs. Previous tests were done on this cantilever which provided the uncoated loss of the cantilever at room temperature and were used in the calculation of the coating loss. The coated sample was tested initially for the loss, but to verify, the chamber was opened and the sample was re-clamped. The impact of the re-clamp is seen below:

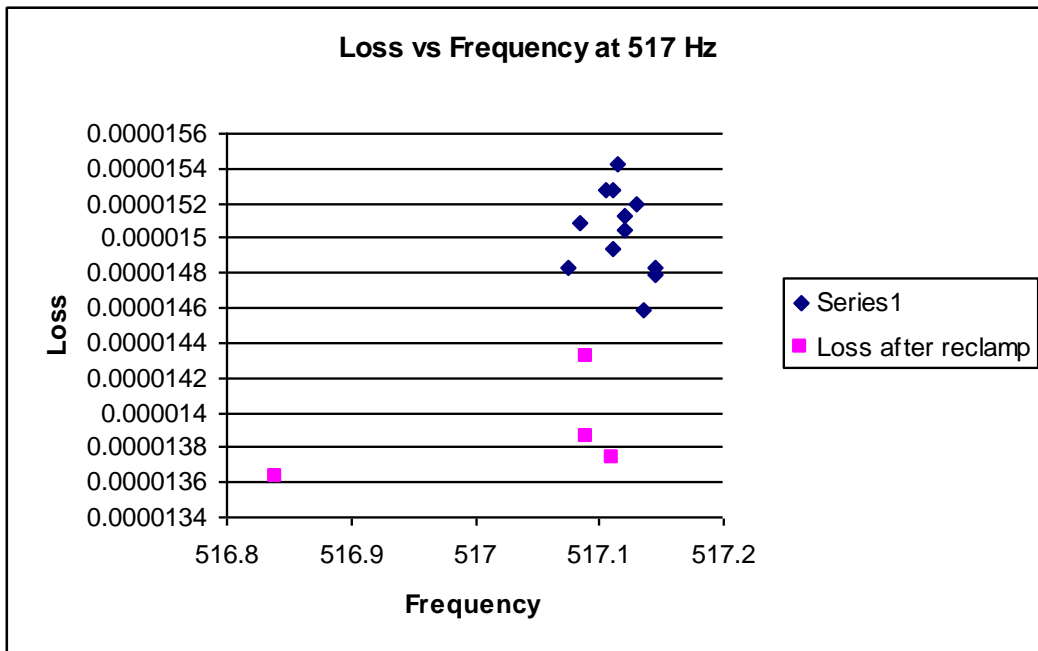


Fig. 17: Impact of re-clamping the silica ribbon coated with tantala at room temperature and 517Hz.

The losses for the total cantilever was 1×10^{-5} , the loss of the coating was to the negative fourth magnitude.

5.3.2 Heated Cantilever

The 500nm tantala coated silica ribbon's loss was found at elevated temperatures of up to 490K. It as found that there was a slight increase in the loss as the temperature increased in the tantala coated silicon ribbon. In addition, the loss was measured on different days to verify the consistency of the measurements as seen in Figs. 18-23.

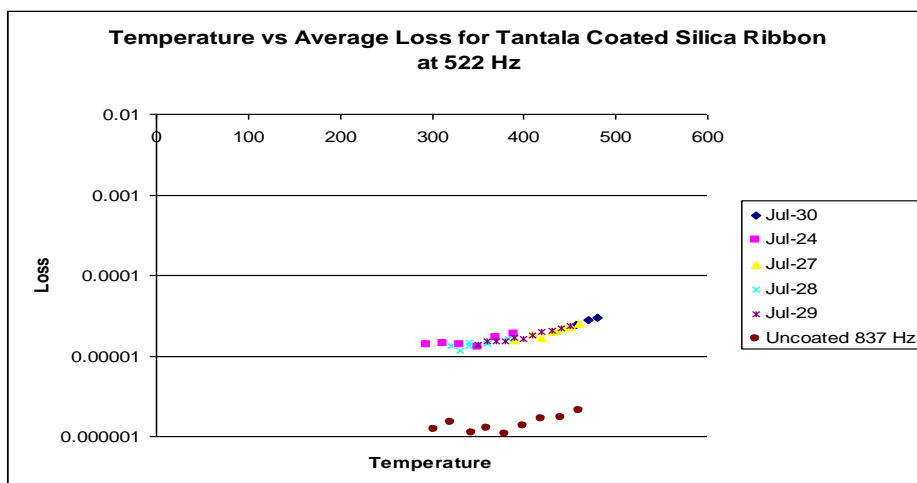


Figure 18: Comparison of the loss for a tantala coated silicon ribbon at resonant mode of 522Hz on different trials, as well as compared to the uncoated loss.

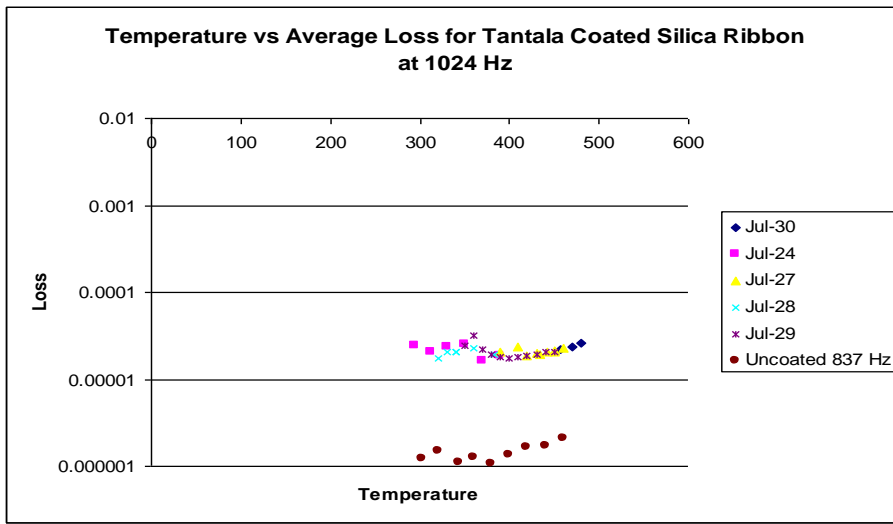


Figure 19: Comparison of the loss for a tantalum coated silicon ribbon at resonant mode of 1024Hz on different trials, as well as compared to the uncoated loss.

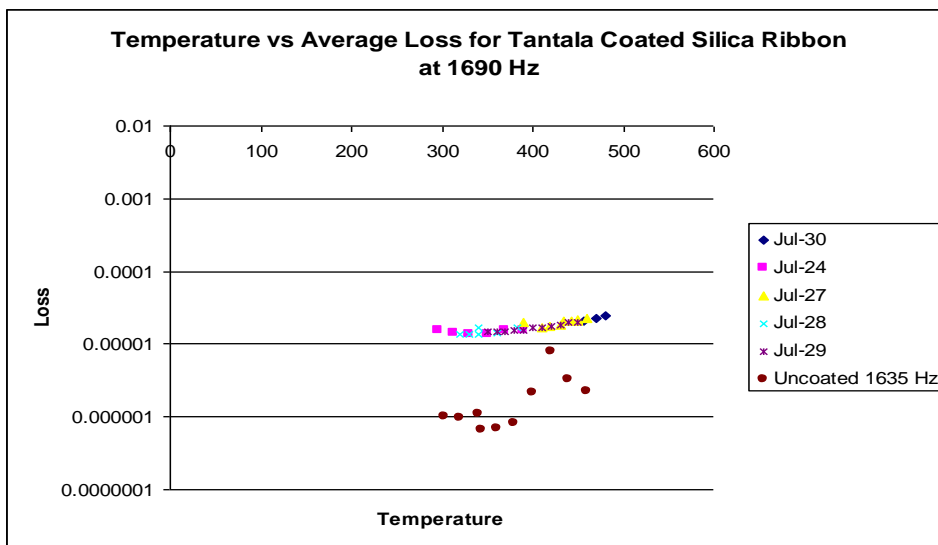


Figure 20: Comparison of the loss for a tantalum coated silicon ribbon at resonant mode of 1690 Hz on different trials, as well as compared to the uncoated loss.

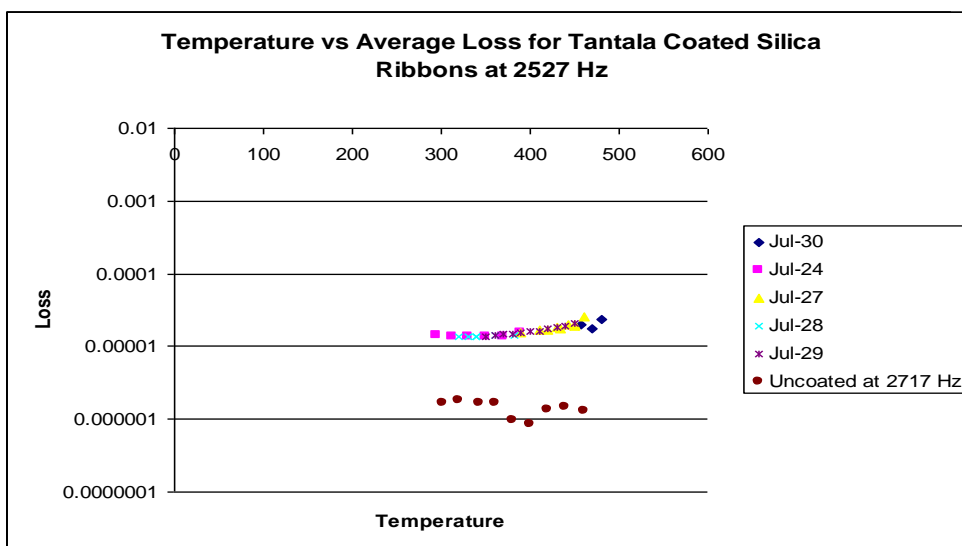


Figure 21: Comparison of the loss for a tantalum coated silicon ribbon at resonant mode of 522Hz on different trials, as well as compared to the uncoated loss.

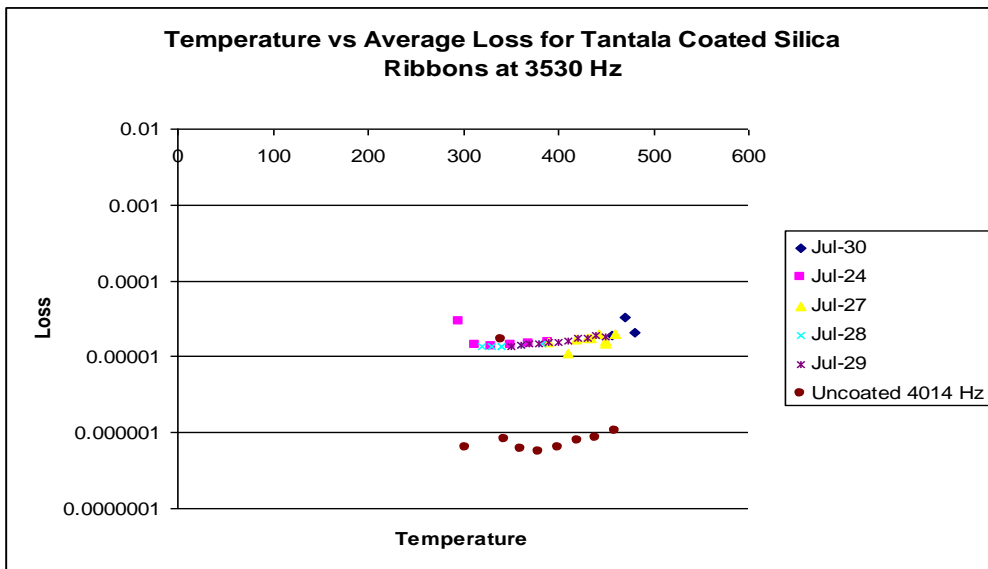


Figure 22: Comparison of the loss for a tantalum coated silicon ribbon at resonant mode of 522Hz on different trials, as well as compared to the uncoated loss.

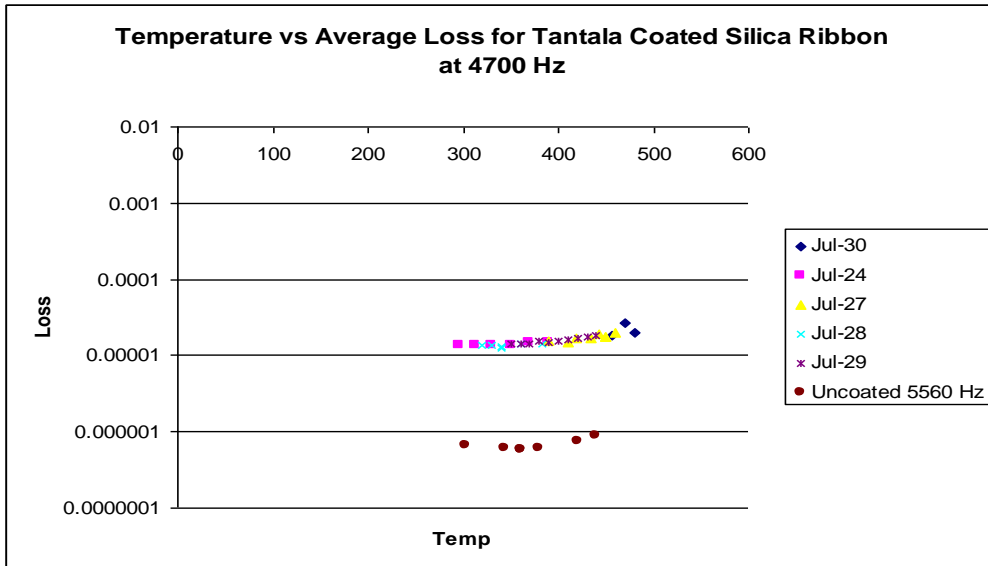


Figure 23: Comparison of the loss for a tantalum coated silicon ribbon at resonant mode of 4700Hz on different trials, as well as compared to the uncoated loss.

5.3.3 Coating Loss

The loss of the tantalum coating was calculated. The actual substrate's loss was not measured at elevated temperatures prior to the coating, so a silica ribbon with equivalent losses was used to model the uncoated losses at elevated temperatures. The loss of the coating was then calculated as outlined in section three. A temperature dependence of loss was found. As the temperature increased, the loss did as well as represented in Fig. 24-29.

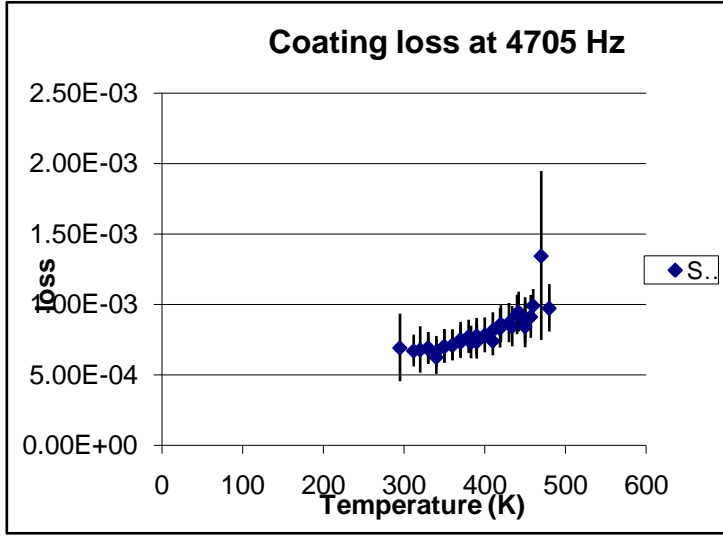


Figure 24: Coating Loss of Tantalum at 4705 Hz

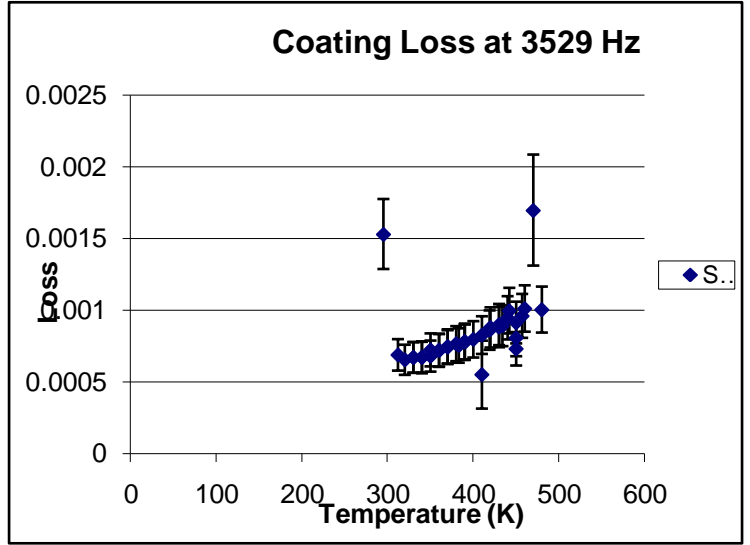


Figure 25: Coating Loss of Tantalum at 3529 Hz

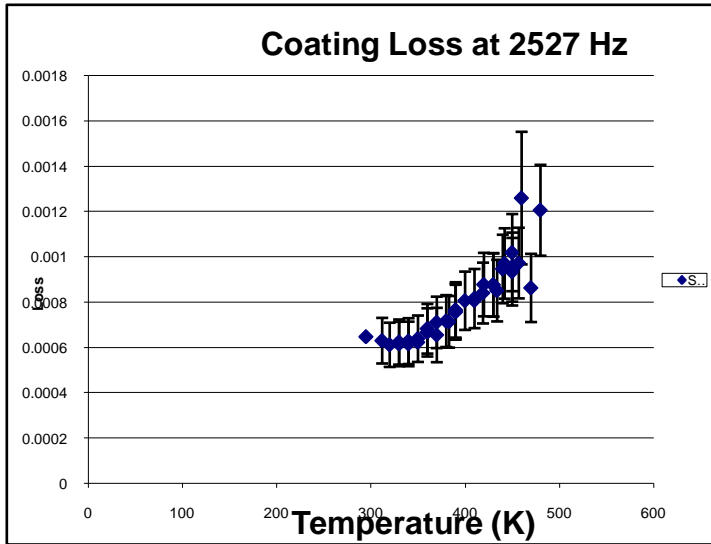


Figure 26: Coating Loss of Tantalum at 4705 Hz

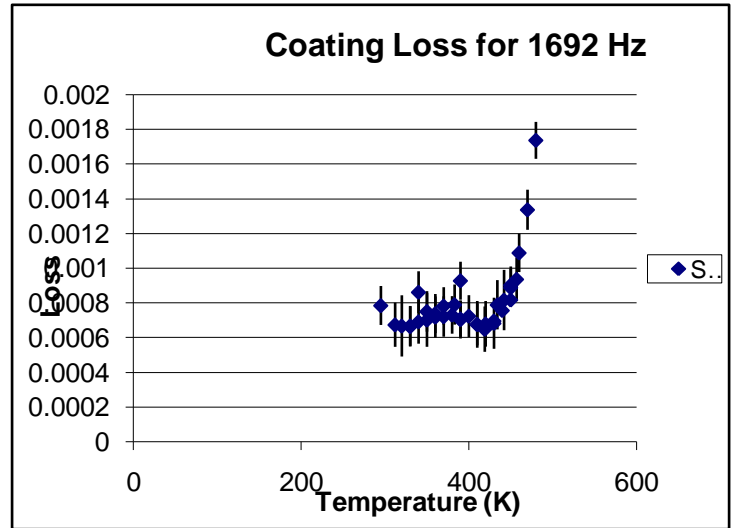


Figure 27: Coating Loss of Tantalum at 1692 Hz

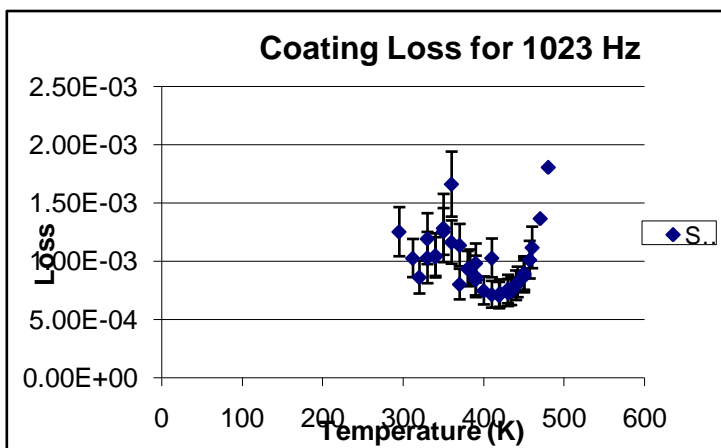


Figure 28: Coating Loss of Tantalum at 4705 Hz

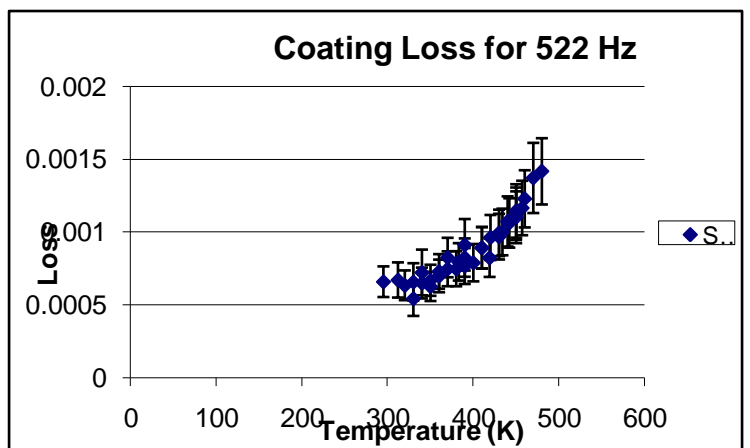


Figure 29: Coating Loss of Tantalum at 1692 Hz

8. Analysis:

Initial measurements found that the silicon cantilever had quite high losses regardless of the tightness of the clamping block. Further measurements on silica provided little better results until the last silica ribbon sample which had very low losses and can be seen in Fig. 11-16. Part of the explanation may be due to the silica samples may have been a bad sample, as each batch can vary. Another possibility is the age of the silica, this could also account for the high losses. Another solution suggested by mentors was the energy coupling. A possible solution was to turn down the bias or off the high voltage after the resonant mode peak was reached. A few of the ring downs occurred too quickly for this to have a large impact as there was not time to turn down the bias.

Further issues were found when the chamber was heated. At one time, the screws became loose when the chamber was heated. This was found when both the uncoated and tantala coated silica ribbon was initially heated. Ring downs were taken, but when the chamber was opened, it was found that the screws that had been initially quite tight were loose. A comparison was done between before the screws were tightened and after the screws were tightened and the difference was for both cantilevers was of significance.

Calculations of the thermo elastic dampening showed that the peak for silicon of 58.5 microns thick at 40Hz. The thermo elastic dissipation was then found for silica 110 microns thick and silicon 72 microns thick. The dissipation peak for silica 110 microns was 270Hz, and the peak for silicon 72 was about 27 KHz.

Calculations of the tantala coating loss provided support for temperature dependence loss. In addition, a peak may occur at higher temperatures although this could not be verified due to the limitations of the experimental set-up. The data suggests that a peak does occur.

9. Conclusion:

Throughout these nine weeks, it was found that the silicon has quite high loss at 300K and above. A problem with the new cantilevers (SiO_2) was the high loss. The silica ribbon has lower loss which is a good sample for coating loss studies. A coated tantala silica ribbon was tested, and the coating had around a 10^{-4} loss which was expected. Addition results found that the loss of the tantala coated silica ribbon increased as the temperature increased. A peak appeared to occur at a temperature higher than 500K in the tantala coating. Verification runs were done to test that the loss of the coated silica ribbon did indeed increase as the temperature increased. It was also found, that an aluminium heating box, not only reduced the temperature gradient within the chamber, but it also allowed the cantilever to be heated to higher temperatures.

Future work may focus at expanding the current set-up for measuring the ring downs as the maximum detected resonant frequency was limited to 56 KHz. In addition, continued measurements of coated cantilever losses' at elevated temperatures may also be determined with additional samples.

10. Acknowledgements

The International Research Experience for Undergraduates is funded in part by National Science Foundation in collaboration with University of Florida and University of Glasgow. Special thanks to Professor Rowan, Director of IGR, and Professor Hough, Associate Director of IGR, for organization and allowance of this research experience as well as Dr. Iain Martin, advisor of my research experience at the IGR lab.

11. References

- [1] J Hough and S. Rowan. *The search for gravitational waves*. Physics World: Einstein 2005, p. 37-41.
- [2] S. Rowan, J. Hough and D.R.M. Crooks. *Thermal noise and material issues for gravitational wave detectors*. Physics Letters A 347 (2005) 25-32.
- [3] G. Benning, C.F.Quate, C.Gerber, Phys. Rev. Lett. 56 (1986)930.
- [4] S. Reid, G. Cagnoli, D.R.M.Crooks, J. Hough, P. Murray, S. Rowan, M.M. Fejer, R. Route, S. Zappe. *Mechanical dissipation in silicon flexures* Phys. Lett. A 351 (2006) 205-11.
- [5] I Martin et. al. *Measurements of a low-temperature mechanical dissipation peak in a single layer of Ta₂O₅ doped with TiO₂*. Classical and Quantum gravity 2008
- [6] I Martin. *Loss measurements using silica at room temperature*. Thesis 2007.
- [7] B.S. Berry, W. C. Prevet. *Vibrating Reed Internal Friction Apparatus Films and Foils*. IBM J. Res. Develop. July 1975.